

Original Research

Electrochemical Removal Kinetics of Nitrate Ions on Copper from Acidic Medium

Fatima Guettari*, Rabah Rehamnia

Laboratoire des Nanomatériaux- Corrosion et Traitements de Surface (LNCTS), Faculté des Sciences, Université Badji Mokhtar, BP 12, Annaba, Algérie

*Received: 24 February 2023**Accepted: 12 June 2023*

Abstract

The electrocatalytic activity of the copper electrode for nitrate electroreduction was performed in acidic medium. The mechanism of the reduction reaction was studied by cyclic voltammetry. One cathodic peak was detected at ca. -0.62 V/SCE, where the charge transfer reaction takes place. The number of electrons involved in the corresponding potential was determined to be eight. The rate-determining step was concluded to be the reduction of nitrate to nitrogen dioxide. According to further analysis, the reduction reaction of NO_3^- on the copper electrode proved to be an irreversible process, with diffusion as its limiting factor. At low concentrations ($[\text{NO}_3^-] \leq 0.1 \text{ M}$), nitrate removal follows first-order kinetics, while it approaches zero at high concentrations ($[\text{NO}_3^-] \geq 0.1 \text{ M}$). As a result, the adsorption phenomena associated with the nitrate reduction process follow a Langmuir isotherm adsorption with a -5.0 KJ mol^{-1} adsorption Gibbs free energy. The charge transfer due to nitrate reaction and hydrogen evolution was further verified by EIS measurements at different potentials, where the diffusion of nitrate ions limits the reaction process. Bulk electrolysis results revealed that current density has a significant effect on nitrate removal efficiency, as well as a percentage of nitrate destruction of up to 88% after 2h, indicating the high capacity of copper for nitrate removal.

Keywords: pollution, copper, kinetics, nitrate removal, electrolysis

Introduction

Over the recent decades, nitrate pollution in ground and surface water has become a common and increasing problem in numerous countries worldwide. This contamination is due to the extensive use of nitrogen based-fertilizers [1-3], which jeopardizes its viability as a source of drinking water [4]. Excess nitrate in drinking water can cause serious health problems [5],

leading to ischemic heart disease [6], cancer [7, 8], multiple sclerosis [9], Non-Hodgkin lymphoma among other conditions [10], and methemoglobinemia or “blue baby syndrome” [11]. For this reason, the threshold value in drinking water is established by the World Health Organization at 50 mg/L, which equates to 11 mg/L of nitrogen coming from nitrate [12, 13].

Several physicochemical processes, such as biological denitrification [14], adsorption [15, 16], coagulation [17], reverse osmosis [18], ion exchange [19] and catalytic reduction [20], are used for nitrate degradation. During the last decade, electrochemical denitrification methods, including principally electro dialysis [21],

*e-mail: fatima.guettari@univ-annaba.org

electrocoagulation [22], and electroreduction [23], have been proposed in environmental technologies. Electrochemical process could be applied to remove nitrate from water. Nitrate is then reduced to different products such as NO_2 , NO_2^- , NO , N_2O , N_2 , NH_2OH , NH_3 , and NH_2NH_2 [24]. These techniques have superior advantages in convenience, environmental friendliness, selectivity, safety and cost-effectiveness.

The mechanism of nitrate electroreduction is very complicated and strongly dependent on experimental conditions like the electrode material [4, 25], cell configuration [26, 27], electrolyte concentration [28], electrolyte composition [4], applied cathodic potential and the presence of other anions in solution [29, 30].

A wide variety of metallic electrodes, such as Pt [31, 32], Pd [3], Cu [30, 33-37], have since been investigated in acidic [31, 32, 34], alkaline [3, 30, 35, 37] and neutral solutions [33, 35, 36]. It appears that Cu exhibited a high activity for nitrate reduction. However, the mechanism of electrochemical reactions has remained less studied. For this reason, this work aims to investigate the nitrate reduction pathway to determine the conditions that allow high efficiency and selectivity of the reaction product.

Experimental

Electrochemical Measurements

Cyclic voltammetry and impedance measurements were carried out with a potentiostat/galvanostat voltalab 40 type PGZ301 (Radiometer Analytical) at room temperature (293 K) using a two-compartment electrochemical cell. The working electrode was a polycrystalline copper disk with 99.9% purity (0.26 cm²) embedded in a resin cylinder. A platinum wire of 0.1 cm² and a saturated calomel electrode (SCE) were used as counter and reference electrodes, respectively.

All working solutions containing 0.5 M H₂SO₄ + xM NaNO₃ were prepared from distilled water, sulfuric acid (Fluka), and sodium nitrate (Fluka) just before use. The solutions were not de-aerated or unbuffered. The pH of the freshly prepared solution was around 1.7.

Before each test, the working electrode was polished with 2000-grade emery paper, degreased with acetone, cleaned with ethanol, and washed with distilled water. Finally, before each experiment, the system was cycled with a 0.5 M H₂SO₄ solution at a 20 mVs⁻¹ scan rate in the cathodic potential range between -0.3 V and -0.7 V (10 cycles), until stable cyclic voltammograms were obtained. The response corresponding to the last scan was recorded and compared with the response obtained for the potential scans after mechanical polishing of the electrode; this pretreatment is required for the electrode stability check. The cell and all glassware were rinsed with acetone and then ethanol. Finally, they were carefully cleaned with distilled water.

The EIS spectra were recorded in the frequency range from 10⁻² to 10⁴ Hz at several potential values. Impedance data were analyzed with Zview software.

Electrolysis

Galvanostatic electrolysis was performed at various current densities with two-compartment cell. The anode is a platinum plate and the cathode is a metal sheet with an area of 50 cm². The electrolysis was performed during 120 min and the sample of treated solution was collected each 15 minutes to quantify nitrate and ammonia concentrations via UV-Vis spectroscopy (JENWAY 6405 UV/Vis). The variations of nitrate concentration were monitored at a wavelength of 220 nm. The final concentration of ammonia was determined by Nessler method at 420 nm.

The efficiency of nitrate reduction was calculated using the first order kinetics according to the following rate law Equation (1):

$$C_t = C_0 \exp(-kt) \quad (1)$$

Where C_0 is the initial concentration of NO_3^- , and C_t is the concentration of NO_3^- at the time t of electrolysis. The nitrate elimination yield $\tau\%$ was evaluated using Eq. (2):

$$\tau\% = \frac{(C_0 - C_t)}{C_0} \times 100 \quad (2)$$

The ammonia selectivity was evaluated using Eq. (3):

$$\zeta_{NH_3} (\%) = X_i / (C_0 - C_t) \times 100 \quad (3)$$

Where X_i is the concentration of the product NO_4^+ formed at time t .

Results and Discussion

Cyclic Voltammetry

Fig. 1 shows the CV response in 0.5 M H₂SO₄. The figure reveals that no peak appears; only hydrogen evolution is observed at ca. -0.70 V. However, in the presence of 0.01 M NaNO₃, the wave centered at ca. -0.6V is related to the reduction of nitrate. The peak shifted to potentials that are more negative as the scan rate increased; furthermore, no peak was observed while sweeping in the positive direction under all scan rates, as expected for irreversible redox processes.

For a diffusion process, the number of electrons (n) transferred in the overall reaction at potential E_p is deduced by the Nicholson and Shain Equation (4) [38, 39]:

$$I_p = 2,99 \times 10^5 n (n_c \alpha_c)^{1/2} A C_0 D_0^{1/2} v^{1/2} \quad (4)$$

Where C_0 is the bulk nitrate concentration (mol cm^{-3}), v the potential scan rate (Vs^{-1}), D_0 the nitrate diffusion coefficient ($1.4 \times 10^{-5} \text{ cm}^2 \text{ s}^{-1}$) [40], A the electrode surface area (0.26 cm^2), I_p the peak current (A), α_c the charge transfer coefficient, and n_c the number of electrons involved in the rate-determining step.

According to what has been reported in the literature [5, 41], the value of the diffusion coefficient used for the determination of the number n of electrons involved in the overall reaction according to Eq. (1) is $2 \times 10^{-5} \text{ cm}^2 \text{ s}^{-1}$. However, N. Aouina et al. [40] have compared the D values obtained by EIS in different nitrate concentrations with the ones obtained earlier by the diaphragm cell method [42]. Based on that, we choose the value of $1.4 \times 10^{-5} \text{ cm}^2 \text{ s}^{-1}$ obtained for a 10^{-2} M nitrate concentration [40].

The value of the charge transfer coefficient α_c was estimated at 0.48; 0.5 from the following relationship (5) [5, 38]:

$$\left| E_p - E_{p/2} \right| = \frac{47,7}{\alpha_c} \quad (mV) \quad (5)$$

Using the Equation (6) [38], the term $n_c \alpha_c$ can be extracted from the slope of the curve (Fig. 3a) to be 0.41:

$$\left| \frac{dE_p}{d \log v} \right| = \frac{29,6}{n_c \alpha_c} \quad (mV) \quad (6)$$

The number of electrons n_c involved in the rate-determining step was found to be 1. Thus, the first electron transfer of the overall reaction is the conversion of nitrate to nitrogen-dioxide, according to the reaction:

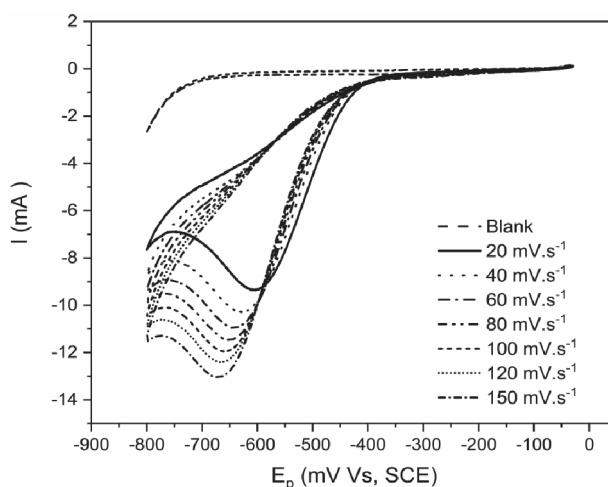
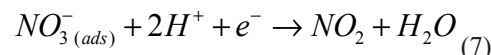


Fig. 1. Cyclic voltammograms on Cu electrode in $0.5 \text{ M H}_2\text{SO}_4 + 0.01 \text{ M NaNO}_3$ at different scan rates. The black curve represents the cycle voltammogram in $0.5 \text{ M H}_2\text{SO}_4$.



From the experimental slope of the linear plot of peak I_p as a function of the square root of scan rate $v^{1/2}$ (Fig. 2b), the number of electrons involved in the overall reaction for a concentration of 0.01 M was estimated at 7.61; 8 electrons.

A few theoretical lines of $-I_p$ vs. $v^{1/2}$ were plotted with a varying number of electron transfer. Diagnostic analysis indicates that one theoretical line had an identical slope to the experimental line, which is in good agreement with the theoretical line constructed for eight electrons. As a result, the only reaction involving eight electrons is the reduction of nitrate to ammonia, as shown in the reaction below.

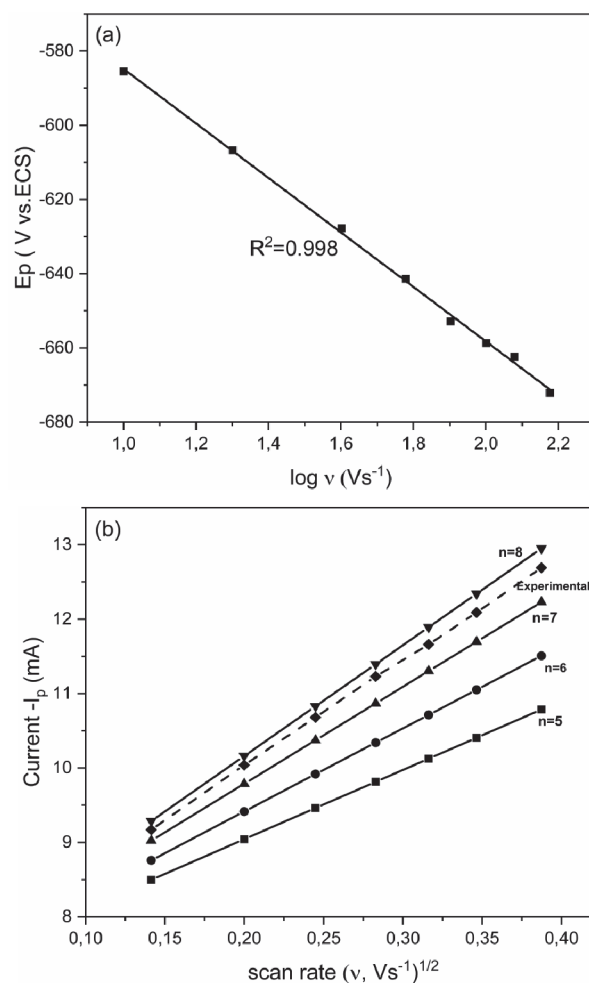
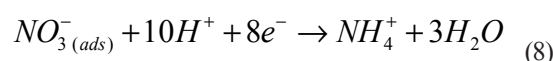
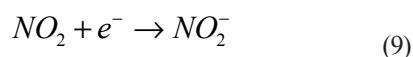
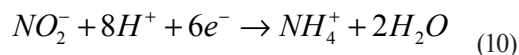


Fig. 2. Scan rate dependent peak potential at Cu electrode in $0.5 \text{ M H}_2\text{SO}_4 + 0.01 \text{ M NaNO}_3$ a). Dependency of peak current on the square root of scan rates. The dashed line for experimentally nitrate reduction and the solid lines represent the theoretically predicted line for 5, 6, 7, and 8 electrons transfer for reduction NO_3^- b).

This leads to propose the following step:



In turn, NO_2^- is reduced according to the reaction:



Thus, we conclude that the ammonium ion is the final product of the electroreduction reaction of the nitrate ion.

Kinetics

In order to elucidate some aspects of the nitrate electroreduction process on a copper electrode, the effect of nitrate concentration on cyclic voltammograms was

evaluated. For low concentrations, such as 10^{-4} M, the current intensity is weak and the peak is large and ill-defined (Fig. 3a). While well-formed peaks are observed for 10^{-3} , 10^{-2} and 10^{-1} M. Furthermore, the peak intensity increases with nitrate concentrations, and reduction of H^+ is shifted to more negative potentials. These results, in agreement with the previous studies [43-45], can be interpreted by considering that the nitrate ions or intermediates are involved in these charge transfer step. Therefore, surface active sites are blocked by nitrate or intermediate species on different metals and media.

Another noteworthy feature of the cyclic voltammograms corresponding to the most concentrated nitrate ion solutions (0.5 M and 1.0 M) is the continual increase in the reduction current and the disappearance of peak and wave. This divergence suggests that the mechanism is different below and above 0.1 M. Also, at low concentrations, sulfate ions occupy a large number of free sites, while at high concentrations, nitrate ions

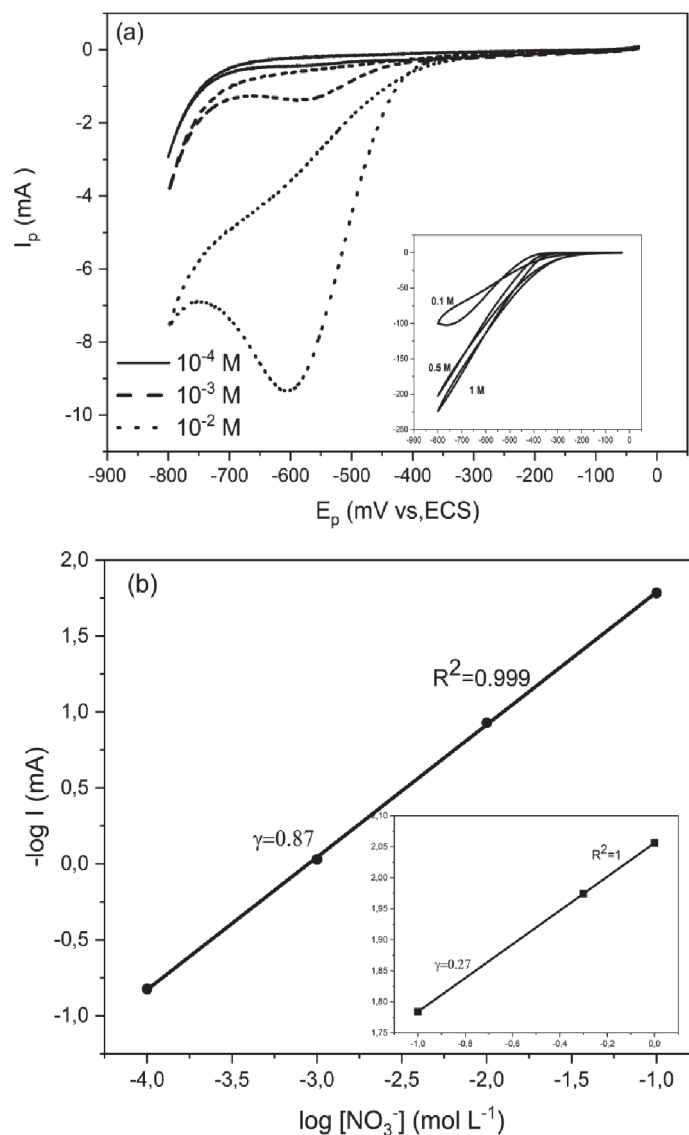


Fig. 3. Cyclic voltammograms of different nitrate concentrations on Cu electrode in 0.5 M H_2SO_4 at scan rate 20 mVs^{-1} a) and $-\log I$ (at fixed potential of -0.60 V) vs $\log [\text{NO}_3^-]$ b).

can compete with SO_4^{2-} ions for available sites [43].

$\log I_p$ (at a fixed potential of ca. -0.6 V) as a function of $\log[\text{NO}_3^-]$ may be expressed by the following equation (11) [44, 46]:

$$\log I_p = \log k + \gamma \log[\text{NO}_3^-] \quad (11)$$

Where k is the kinetic rate constant and γ is the kinetic order. From the straight line, shown in (Fig. 3b), the kinetic order reaction was found to be 0.87 and 0.27 for nitrate concentrations below and above 0.1 M. The reaction order is close to 1, indicating a first-order kinetic, which is in agreement with values obtained by most studies [4, 28, 47]. On the other hand, the kinetic order of value 0.27 shows that at high concentrations of $[\text{NO}_3^-] \geq 0.1$ M, the amount of adsorbed electroactive species is more important. The change in kinetic order as a function of nitrate concentration confirms the adsorption of electroactive species prior to charge transfer.

Clearly, the adsorption-desorption equilibrium limited the overall reduction of nitrate ions. For this reason, its adsorption free energy was calculated.

According to the literature [44, 48], a Langmuir isotherm was adopted to evaluate the nitrate adsorption equilibrium constant, b , which can be determined by the following Equation (12):

$$\frac{[\text{NO}_3^-]}{I_p} = \frac{1}{bI_{p,\max}} + \frac{[\text{NO}_3^-]}{I_{p,\max}} \quad (12)$$

Analysis of the data in Fig. 4 at the copper electrode reveals a linear plot of $\frac{[\text{NO}_3^-]}{I_p}$ versus $[\text{NO}_3^-]$ with a correlation coefficient of 0.99. Thus, the isotherm of Langmuir describes the adsorption of nitrate ions.

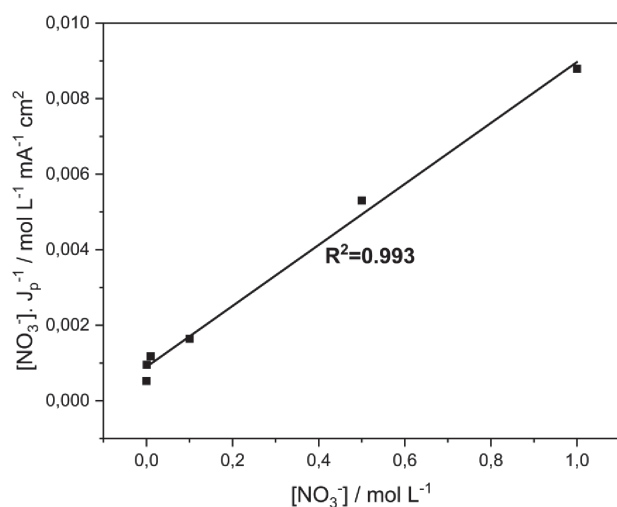


Fig. 4. Langmuir adsorption isotherm of NO_3^- ions on Cu electrode at -0.60 V.

The equilibrium constant b was determined to be ca. 8.01 M^{-1} . The adsorption free energy $\Delta_{ad}G^0$ of NO_3^- ions on Cu was calculated from $\Delta_{ad}G^0 = -RT \ln b$ [44] and estimated at ca. $-5.06 \text{ KJ mol}^{-1}$. This value is lower than the reported one for $\text{Pd}_{33}\text{Ni}_{60}\text{P}_7$ electrode (i.e. -7.3 KJ mol^{-1}) [49].

The results reveal that the copper has catalytic activity for electrochemical nitrate reduction, which requires adsorption of electro-active species onto the electrode surface.

EIS Measurements

Fig. 5 represents the impedance spectra of 0.01 M NaNO_3 in 0.5 M H_2SO_4 at different potentials. The Nyquist plots depend on the frequency of the excitation potential and the possibility of charge transfer. Additionally, the plots were similar and revealed a single capacitive loop near perfect semicircle at high frequencies and linear impedance with an angle of $\approx 50^\circ$ to the real axis at low frequencies. This latter feature is due to relaxations occurring at the electrode-solution interface and indicates a diffusion-controlled charge transfer mechanism, which might be the nitrate towards the surface electrode. At high frequencies, the diameters of the capacitive loops decreased, indicating that charge transfer resistance decreased due to the reaction (1), and because diffusing reactants do not have to move very far, the impedance due to nitrate ions diffusion is low.

The insets of Fig. 5 show the respective equivalent circuits obtained by simulating the experimental Nyquist data with Zview software. The equivalent circuits consist of a constant phase element (CPE1) in series with a solution resistance (R_1) and in parallel with a branch of diffusion, i.e., charge transfer resistance (R_2) and Warburg impedance (W_1). The following

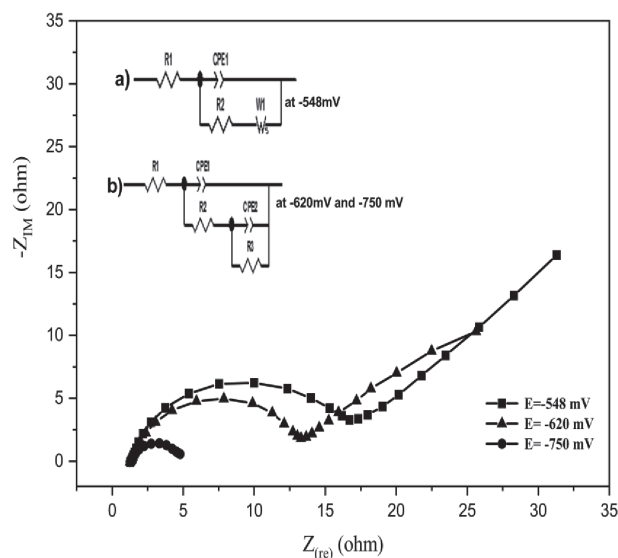


Fig. 5. Nyquist plots of Cu in 0.5M H_2SO_4 + 0.01 M NaNO_3 at different potentials. Insets show the corresponding equivalent circuit to the Nyquist plots.

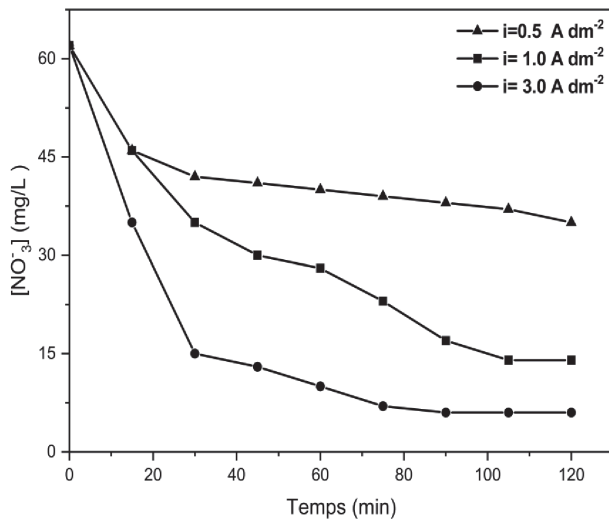


Fig. 6. Effect of current densities on nitrate residual concentration using Cu electrode. The initial concentration of nitrate was 62 mg/L.

equation gives the value of the double layer capacity: $C_{dl} = CPE1(\omega_{max}^{\alpha-1})$, with $\omega = 2\pi f$ (f represents the frequency at which the imaginary value reaches a maximum on the Nyquist diagram). However, the second time is related to the layer's response formed on the surface of the electrode (CPE2, R3). These parameters are grouped in Table 1.

At ca. -0.72 V, the water reduction reaction is favored, which is explained by a significant decrease in the polarization resistance. The low value of polarization resistance is attributed to the blocking of surface sites by hydrogen, which inhibits the diffusion of nitrate ions towards the surface.

On the other hand, the SIE diagrams obtained in a 0.5 M H₂SO₄ acid medium at different NaNO₃ concentrations (data not shown) clearly show that whatever the nitrate concentration, the relaxation time linked to the diffusion is observed. Although, based on polarization resistance values, it appears that at moderate nitrate concentrations, reduction is favored while it is retarded at high concentrations. These results confirm those obtained in section 3.1.

Bulk Electrolysis

In order to evaluate the activity of the copper towards the nitrate reduction reaction and quantify the yield of

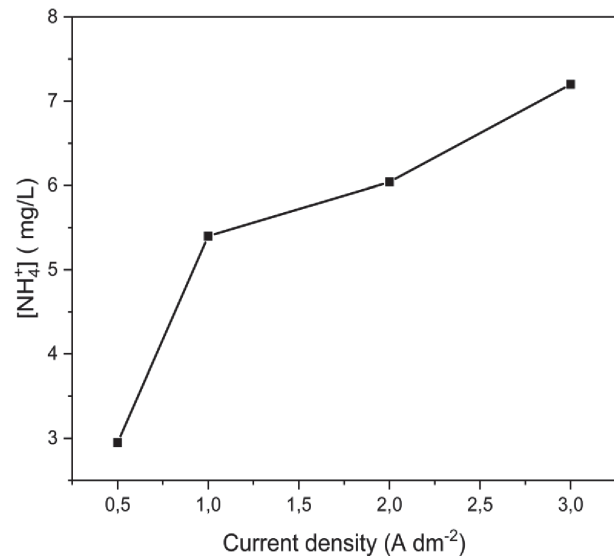


Fig. 7. Variation of ammonia concentration at different current densities formed onto Cu electrode and 62 mg/L of NO₃⁻.

the reaction, galvanostatic electrolysis (0.5÷3.0 A dm⁻²) was carried out for 120 min in freshly prepared solutions with an initial nitrate concentration of 62 mg/L.

The results in Fig. 6 showed a decrease in the final nitrate concentration when electrolysis time increased at all current densities.

During electrolysis at 0.5 A dm⁻², it appears that the reduction of nitrate is low, and the acceptable limit was not reached after 120 min. While, the initial nitrate concentration of 62 mg/L could achieve the WHO guideline value of 25 mg/L during 2 hours of electrolysis for 1.0 A dm⁻² and 3.0 A dm⁻² with maximum removals of nitrate of 75.73 % and 88.06 %, achieved up to 120 min, respectively.

Moreover, for both current densities, the removal efficiency increased with time during the first 30 min to become very slow for the rest of the electrolysis. The same observation is applicable to the conversion rate, which reaches 77.16 % after 30 min for 3.0 A dm⁻², which is greater than the value obtained after 120 min for a current density of 1.0 A dm⁻². By comparing the efficiency values of electrolysis at all current densities, we found that the copper electrode is useful for eliminating nitrate by electrochemical treatment. The current density determines the rate reduction. The values of first order rate constants were estimated as

Table 1. Physical parameters deduced from EIS measurement performed at different potentials.

Potential (mV)	R ₁ (Ω.cm ²)	CPE ₁ (F cm ⁻² s ^(1-α))	α ₁	R ₂ (Ω.cm ²)	CPE ₂	α ₂	R3 (Ω.cm ²)
-548	1.39	1.71 10 ⁻⁴	0.889	14.21	W ₁ = 81.82		
-620	1.38	1.726 10 ⁻⁴	0.878	11.82	6.83 10 ⁻²	0.628	43.44
-720	1.435	1.0713 10 ⁻⁴	0.93	3.15	8.389 10 ⁻³	0.8667	0.826

0.00145, 0.0112, and 0.0129 min⁻¹ for 0.5, 1, and 3 A dm⁻², respectively. The nitrate could be removed through an electrochemical process by first-order kinetics; this result is in agreement with those obtained in kinetics section.

The analysis of NH₄⁺ at different current densities, as shown in Fig. 7, indicates that ammonia concentration increased from 2.95 to 7.2 mg/L, corresponding to a percentage of ammonia formation up to 45%. This result requires optimization of the electrolysis parameters to improve the copper electrode selectivity.

Conclusions

In this study, the electrochemical reduction of nitrate ions was investigated on copper in 0.5 M H₂SO₄. The reaction shows a single wave centered at -0.60 V vs. SCE, which is undoubtedly due to the reduction of NO₃⁻. The rate-determining step was found to be the reduction of NO₃⁻ to NO₂, which is in accordance with some previous studies [50], and in contrast with [30, 51], where the limiting step involves 2 electrons, i.e., from NO₃⁻ to NO₂⁻. Then a one-electron step corresponding to the conversion of NO₂ to NO₂⁻ was followed by a third six-electron step to produce NH₄⁺. Thus, a mechanism was proposed, where the final product of electroreduction of NO₃⁻ is ammonium ions. The cyclic voltammograms revealed that NO₃⁻ adsorption follows the Langmuir isotherm, which is a required step for electrochemical processes. The order of the reaction depends on the NO₃⁻ concentration. It decreases from 0.87 ([NO₃⁻] ≤ 0.1 M) to 0.27 ([NO₃⁻] ≥ 0.1 M). Galvanostatic electrolysis during 2 hours shows a nitrate conversion up to 75.53 % and 88.06 % for densities current of 1.0 and 3.0 A.dm⁻², respectively. Process efficiency increases with increasing current densities, and 30 min of treatment at 3 A.dm⁻² proved to be enough in order to remove nitrate almost entirely (88.06%). NH₄⁺, as a reaction product, can reach a percentage formation of up to 45 %.

Acknowledgments

This work is supported by the General Directorate for Scientific Research and Technological Development (DG-RSDT), Algerian Ministry of Scientific Research, Algeria.

Conflict of Interest

The authors declare that they have no known competing financial interests or personal relationships that could have appeared to influence the work reported in this paper.

The authors received no financial support for the authorship, and/or publication of this article.

References

- SINGH N., GOLDSMITH B.R. Role of Electrocatalysis in the Remediation of Water Pollutants. *ACS Catal.* **10** (5), 3365, **2020**.
- VAN LANGEVELDE P.H., KASTOUNAROS I., KOPER M.T.M. Electrocatalytic Nitrate Reduction for Sustainable Ammonia Production. *Joul.* **5** (2), 290, **2021**.
- LIM J., LIU C.Y., PARK J., LIU Y.H., SENFTLE T.P., LEE S.W., HATZELL M.C. Structure Sensitivity of Pd Facets for Enhanced Electrochemical Nitrate Reduction to Ammonia. *ACS Catal.* **11** (12), 7568, **2021**.
- ORIOLO R., BRILLAS E., CABOT P.L., CORTINA J.L., SIREN I. Paired electrochemical removal of nitrate and terbuthylazine pesticide from groundwater using mesh electrodes. *Electrochim. Acta.* **383** (3), 138354, **2021**.
- SU J.F., RUZYBAYEV I., SHAH I., HUANG C.P. The electrochemical reduction of nitrate over micro-architected metal electrodes with stainless steel scaffold. *Appl. Catal. B Environ.* **180** (1), 199, **2016**.
- PRAGANI M.A., DESAI K.P., MORRONE D., SIDHU M.S., BODEN W.E. The role of nitrates in the management of stable ischemic heart disease: A review of the current evidence and guidelines. *Rev. Cardiovasc. Med.* **18** (1), 14, **2017**.
- WARD M., JONES R., BRENDER J., DE KOK T., WEYER P., NOLAN B., VILLANUEVA C., VAN BREA S. Drinking Water Nitrate and Human Health: An Updated Review. *International Journal of Environmental Research and Public Health.* **15** (7), 1557, **2018**.
- JONES R.R., WEYER P.J., DELLAVALLE C.T., INOUE-CHOI M., ANDERSON K.E., CANTOR K.P., KRASNER S., ROBIEN K., BEANE FREEMAN L.E., SILVERMAN D.T., WARD M.H. Nitrate from drinking water and diet and bladder cancer among postmenopausal women in Iowa. *Environ. Health Perspect.* **124** (11), 1751, **2016**.
- ZHAI Y., ZHAO X., TENG Y., LI X., ZHANG J., WU J., ZUO R. Groundwater nitrate pollution and human health risk assessment by using HHRA model in an agricultural area, NE China. *Ecotoxicol. Environ. Saf.* **137**, 130, **2017**.
- ROJAS FABRO A.Y., PACHECO AVILA J.G., ESTELLER ALBERICH M.V., CABRERA SANORES S.A., CAMARGO-VALERO M.A. Spatial distribution of nitrate health risk associated with groundwater use as drinking water in Merida, Mexico. *Appl. Geogr.* **65**, 49, **2015**.
- PARVIZISHAD M., DALVAND A., MAHVI A.H., GOODARZI F. A Review of Adverse Effects and Benefits of Nitrate and Nitrite in Drinking Water and Food on Human Heal. *Health Scope.* **6** (3), **2017**.
- WHO: Nitrate and nitrite in drinking water. **2016**.
- WHO: Guidelines for drinking-water quality. **2017**.
- LI X. M., CHEN H. B., YANG Q., WANG D. B., LUO K., ZENG G.M. Biological nutrient removal in a sequencing batch reactor operated as oxic/anoxic/extended-idle regime. *Chemosphere.* **105**, 75, **2014**.
- ZHOU H., TAN Y., GAO W., ZHANG Y., YANG Y. Selective nitrate removal from aqueous solutions by a hydrotalcite-like absorbent FeMgMn-LDH. *Sci. Rep.* **10** (1), 1, **2020**.
- MALAKOOTIAN M., YAGHMAEIAN K., HASHEMI S.Y., FARPOOR M.H. Evaluation of Clay Soil Efficacy Carrying Zero-Valent Iron Nanoparticles to Remove Nitrate From Aqueous Solutions. *J. Water Chem. Technol.* **41** (1), 29, **2019**.

17. AGHAPOUR A.A., NEMATI S., MOHAMMADI A., NOURMORADI H., KARIMZADEH S. Nitrate removal from water using alum and ferric chloride: A comparative study of alum and ferric chloride efficiency. *Environ. Heal. Eng. Manag.* **3** (2), 69, **2016**.
18. EPSZTEIN R., NIR O., LAHAV O., GREEN M. Selective nitrate removal from groundwater using a hybrid nanofiltration-reverse osmosis filtration scheme. *Chem. Eng. J.* **279**, 372, **2015**.
19. CHOE J.K., BERGQUIST A.M., JEONG S., GUEST J.S., WERTH C.J., STRATHMANN T.J. Performance and life cycle environmental benefits of recycling spent ion exchange brines by catalytic treatment of nitrate. *Water Res.* **80**, 267, **2015**.
20. HUO X., VAN HOOMISSEN D.J., LIU J., VYAS S., STRATHMANN T.J. Hydrogenation of aqueous nitrate and nitrite with ruthenium catalysts. *Appl. Catal. B Environ.* **211**, 188, **2017**.
21. BOSKO M.L., RODRIGUES M.A.S., FERREIRA J.Z., MIRÓ E.E., BERNARDES A.M. Nitrate reduction of brines from water desalination plants by membrane electrolysis. *J. Memb. Sci.* **451**, 276, **2014**.
22. GUO M., FENG L., LIU Y., ZHANG L. Electrochemical simultaneous denitrification and removal of phosphorus from the effluent of a municipal wastewater treatment plant using cheap metal electrodes. *Environ. Sci. Water Res. Technol.* **6** (4), 1095, **2020**.
23. GAO J., SHI N., LI Y., JIANG B., MARHABA T., ZHANG W. Electrocatalytic upcycling of nitrate wastewater into an ammonia fertilizer via an electrified membrane. *Environ. Sci. Technol.* **56** (16), 11602, **2022**.
24. DORTISIOU M., KYRIACOU G. Electrochemical reduction of nitrate on bismuth cathodes. *J. Electroanal. Chem.* **630** (1-2), 69, **2009**.
25. FAJARDO A.S., WESTERHOFF P., SANCHEZ-SANCHEZ C.M., GARCIA-SEGURA S. Earth-abundant elements a sustainable solution for electrocatalytic reduction of nitrate. *Appl. Catal. B Environ.* **281**, 119465, **2021**.
26. DING J., LI W., ZHAO Q.L., WANG K., ZHENG Z., GAO Y.Z. Electroreduction of nitrate in water: Role of cathode and cell configuration. *Chem. Eng. J.* **271**, 252, **2015**.
27. LI W., XIAO C., ZHAO Y., ZHAO Q., FAN R., XUE J. Electrochemical reduction of high-concentrated nitrate using Ti/TiO₂ nanotube array anode and Fe cathode in dual-chamber cell. *Catal. Letters.* **146** (12), 2585, **2016**.
28. KATSOUNAROS I., KYRIACOU G. Influence of nitrate concentration on its electrochemical reduction on tin cathode: Identification of reaction intermediates. *Electrochim. Acta.* **53** (17), 5477, **2008**.
29. SZPYRKOWICZ L., DANIELE S., RADAELLI M., SPECCHIA S. Removal of NO₃⁻ from water by electrochemical reduction in different reactor configurations. *Appl. Catal. B Environ.* **66** (1-2), 40, **2006**.
30. REYTER D., BÉLANGER D., ROUÉ L. Study of the electroreduction of nitrate on copper in alkaline solution. *Electrochim. Acta.* **53** (20), 5977, **2008**.
31. MOLODKINA E.B., BOTRYAKOVA I.G., DANILOV A.I., SOUZA-GARCIA J., FIGUEIREDO M.C., FELIU J.M. Redox transformations of adsorbed NO molecules on Pt(100) electrode. *Russ. J. Electrochem.* **50** (21), 8, **2015**.
32. EHRENBURG M.R., DANILOV A.I., BOTRYAKOVA I.G., MOLODKINA E.B., RUDNEV A. V. Electroreduction of nitrate anions on cubic and polyoriented platinum nanoparticles modified by copper adatoms. *J. Electroanal. Chem.* **802**, 109, **2017**.
33. MALINOVIC B.N., PAVLOVIC M.G., HALILOVIC N. Electrochemical removal of nitrate from wastewater using copper cathode. *J. Environ. Prot. Ecol.* **16** (4), 1273, **2015**.
34. ÇIRMI D., AYDIN R., KÖLELİ F. The electrochemical reduction of nitrate ion on polypyrrole coated copper electrode. *J. Electroanal. Chem.* **736**, 101, **2015**.
35. COMISSO N., CATTARIN S., GUERRIERO P., MATTAROZZI L., MUSIANI M., VÁZQUEZ-GÓMEZ L., VERLATO E. Study of Cu, Cu-Ni and Rh-modified Cu porous layers as electrode materials for the electroanalysis of nitrate and nitrite ions. *J. Solid State Electrochem.* **20** (4), 1139, **2016**.
36. ABDALLAH, R., GENESTE F., LABASQUE T., DJELAL H., FOURCADE F., AMRANE A., TAHA S., FLONER D. Selective and quantitative nitrate electroreduction to ammonium using a porous copper electrode in an electrochemical flow cell. *J. Electroanal. Chem.* **727**, 148, **2014**.
37. BADEA G.E. Electrocatalytic reduction of nitrate on copper electrode in alkaline solution. *Electrochim. Acta.* **54** (3), 996, **2009**.
38. BRETT C.M.A., BRETT A.M.O. *Electrochemistry: Principles, methods, and applications*, 1st ed.; Oxford University Press: New York, Unites States, **1993**.
39. BARD A.J., FAULKNER L.R. *Electrochemical: Methods Fundamentals and Applications*, 2nd ed.; Wiley: New York, United States, **2000**.
40. AOUIA N., CACHET H., DEBIEMME-CHOUVY C., TRAN T.T.M. Insight into the electroreduction of nitrate ions at a copper electrode, in neutral solution, after determination of their diffusion coefficient by electrochemical impedance spectroscopy. *Electrochim. Acta.* **55** (24), 7341, **2010**.
41. HASNAT M.A., RASHED M.A., BEN AOUN S., UDDIN S.M.N., SAIFUL ALAM M., AMERTHARAJ S., MAJUMDER R.K., MOHAMED N. Dissimilar catalytic trails of nitrate reduction on Cu-modified Pt surface immobilized on H⁺ conducting solid polymer. *J. Mol. Catal. A Chem.* **383–384**, 243, **2014**.
42. HARNED H.S., SHROPSHIRE J.A. The Diffusion and Activity Coefficient of Sodium Nitrate in Dilute Aqueous Solutions at 25°. *J. Am. Chem. Soc.* **80** (11), 2618, **1958**.
43. DE GROOT M.T., KOPER M.T.M. The influence of nitrate concentration and acidity on the electrocatalytic reduction of nitrate on platinum. *J. Electroanal. Chem.* **562** (1), 81, **2004**.
44. HASNAT M.A., BEN AOUN S., NIZAM UDDIN S.M., ALAM M.M., KOAY P.P., AMERTHARAJ S., RASHED M.A., RAHMAN M.M., MOHAMED N. Copper-immobilized platinum electrocatalyst for the effective reduction of nitrate in a low conductive medium: Mechanism, adsorption thermodynamics and stability. *Appl. Catal. A Gen.* **478**, 259, **2014**.
45. KOAY P.P., ALAM M.S., ALAM M.M., ETESAMI M., HASNAT M.A., MOHAMED N. Electrocatalytic reduction of nitrate ions at a poly crystalline SnCu modified platinum surface by using an H⁺ conducting solid polymer in a sandwich type membrane reactor. *J. Environ. Chem. Eng.* **4** (4), 4494, **2016**.
46. YIN D., LIU Y., SONG P., CHEN P., LIU X., CAI L., ZHANG L. In situ growth of copper/reduced graphene oxide on graphite surfaces for the electrocatalytic reduction of nitrate. *Electrochimica Acta.* **324**, 134846, **2019**.
47. REYTER D., CHAMOULAUD G., BÉLANGER D., ROUÉ L. Electrocatalytic reduction of nitrate on copper

- electrodes prepared by high-energy ball milling. *Journal of Electroanalytical Chemistry*. **596** (1), 13, **2006**.
48. KHAIRY M., KAMPOURIS D.K., KADARA R.O., BANKS C.E. Gold Nanoparticle Modified Screen Printed Electrodes for the Trace Sensing of Arsenic(III) in the Presence of Copper(II). *Electroanalysis*. **22** (21), 2496, **2010**.
49. LOU Y., SHAO Y.T., LI P., LI Z.L., NIU Z.J. Electrocatalytic reduction of NO_3^- in a neutral solution on an electrodeposited film of amorphous Pd₃₃Ni₆₀P₇ alloy. *Journal of Electroanalytical Chemistry*. **624** (1-2), 33, **2008**.
50. SU J.F., RUZYBAYEV I., SHAH I., HUANG C.P. The electrochemical reduction of nitrate over micro-architected metal electrodes with stainless steel scaffold. *Applied Catalysis B: Environmental*. **180** (1), 199, **2016**.
51. DIMA G.E., DE VOOYS A.C.A., KOPER M.T.M. Electrocatalytic reduction of nitrate at low concentration on coinage and transition-metal electrodes in acid solutions. *Journal of Electroanalytical Chemistry*. **554–555** (1), 15, **2003**.